The Journal of Immunology

MicroRNA-494 Is Required for the Accumulation and Functions of Tumor-Expanded Myeloid-Derived Suppressor Cells via Targeting of PTEN

Yang Liu, Lihua Lai, Qingyun Chen, Yinjing Song, Sheng Xu, Feng Ma, Xiaojian Wang, Jianli Wang, Hai Yu, Xuetao Cao and Qingqing Wang

J Immunol 2012; 188:5500-5510; Prepublished online 27 April 2012;
doi: 10.4049/jimmunol.1103505
http://www.jimmunol.org/content/188/11/5500

The Journal of Immunology is published twice each month by
The American Association of Immunologists, Inc.,
1451 Rockville Pike, Suite 650, Rockville, MD 20852

Print ISSN: 0022-1767 Online ISSN: 1550-6606.

MicroRNA-494 Is Required for the Accumulation and Functions of Tumor-Expanded Myeloid-Derived Suppressor Cells via Targeting of PTEN

Yang Liu,*,[1] Lihua Lai,*,[1] Qingyun Chen,*,[1] Yinjing Song,* Sheng Xu,[†,‡] Feng Ma,[†,‡] Xiaojian Wang,* Jianli Wang,* Hai Yu,* Xuetao Cao,*,[†,‡] and Qingqing Wang*

Myeloid-derived suppressor cells (MDSCs) potently suppress the anti-tumor immune responses and also orchestrate the tumor microenvironment that favors tumor angiogenesis and metastasis. The molecular networks regulating the accumulation and functions of tumor-expanded MDSCs are largely unknown. In this study, we identified microRNA-494 (miR-494), whose expression was dramatically induced by tumor-derived factors, as an essential player in regulating the accumulation and activity of MDSCs by targeting of phosphatase and tensin homolog (PTEN) and activation of the Akt pathway. TGF-β1 was found to be the main tumor-derived factor responsible for the upregulation of miR-494 in MDSCs. Expression of miR-494 not only enhanced CXCR4-mediated MDSC chemotaxis but also altered the intrinsic apoptotic/survival signal by targeting of PTEN, thus contributing to the accumulation of MDSCs in tumor tissues. Consequently, downregulation of PTEN resulted in increased activity of the Akt pathway and the subsequent upregulation of MMPs for facilitation of tumor cell invasion and metastasis. Knockdown of miR-494 significantly reversed the activity of MDSCs and inhibited the tumor growth and metastasis of 4T1 murine breast cancer in vivo. Collectively, our findings reveal that TGF-β1–induced miR-494 expression in MDSCs plays a critical role in the molecular events governing the accumulation and functions of tumor-expanded MDSCs and might be identified as a potential target in cancer therapy. *The Journal of Immunology*, **2012, 188: 5500–5510.**

Accumulating evidence indicates that tumor-infiltrating inflammatory cells contribute significantly to tumor progression by suppressing host immunity, facilitating tumor cell invasion, and participating in the formation of new blood vessels (1, 2). Suppressive myeloid cells were described >20 y ago in cancer patients (3), but their functional importance in regulating the immune response and tumor development has only been appreciated in recent years. It has now been consistently shown in many studies that a population of cells with suppressive activity (known as myeloid-derived suppressor cells; MDSCs) contributes to the negative regulation of immune responses during cancer and other diseases (4). MDSCs represent a heterogeneous population of myeloid cells in early differential stages that can be identified in mice by expression of CD11b and Gr-1 (4). More recently, tumor-expanded MDSCs were subdivided into two different subsets based on their expression of the two molecules Ly-6C and Ly-6G: granulocytic MDSCs ($CD11b^{+}Ly6C^{low}Ly6G^{high}$) and monocytic MDSCs ($CD11b^{+}Ly6G^{low}Ly6C^{high}$) (5, 6).

As one of the main cell populations responsible for regulating immune responses, MDSCs act to suppress T cell function through a number of mechanisms involving arginase 1 (ARG1), inducible NO synthase, and reactive oxygen species (4, 7). The expansion of MDSCs is regulated by several factors released by tumor cells, stromal cells, and activated immune cells; these factors trigger different signaling pathways in MDSCs that mainly involve the STAT family of transcription factors, including STAT1, STAT3, and STAT6 (4, 8). Besides suppression of T cell response, we also found that MDSCs could induce NK cell anergy (9).

In addition to their depressive effect on host immune surveillance, MDSCs also play critical roles in prompting of tumor invasion and metastasis (5, 6). We and others have previously reported that tumor-derived factors mobilize MDSCs from the bone marrow into the tumor site where they produce multiple MMPs that contribute to tumor invasion (10, 11). The regulation of adaptive immune response by MDSCs has been extensively studied. It has become clear that the immunosuppressive activity of MDSCs requires the persistent activation of STAT3 (4, 12); however, the molecular mechanisms that regulate the accumulation and activity of MDSCs especially the nonimmunological functions still remain to be elucidated. Understanding the molecular networks controlling the accumulation and functional determination of MDSCs is essential in identifying potential therapeutic targets for cancer intervention.

*Institute of Immunology, Zhejiang University School of Medicine, Hangzhou 310058, People's Republic of China; †National Key Laboratory of Medical Immunology, Second Military Medical University, Shanghai 200433, People's Republic of China; and ‡Institute of Immunology, Second Military Medical University, Shanghai 200433, People's Republic of China

[1]Y.L., L.L., and Q.C. contributed equally to this work.

Received for publication December 6, 2011. Accepted for publication April 3, 2012.

This work was supported by grants from the National Natural Science Foundation of China (30872377 and 81072405), the Program for New Century Excellent Talents in University from the Ministry of Education of the People's Republic of China (NCET-08-0486), and a grant from the Zhejiang Provincial Natural Science Foundation (R2100528). This work was also supported by the Zhejiang Provincial Program for the Cultivation of High-Level Innovative Health Talents, Innovative Research Team (2010R50046) and the Zhejiang Major Science and Technology Special Project (2009C13018).

The microarray data presented in this article have been submitted to the Gene Expression Omnibus (http://www.ncbi.nlm.nih.gov/geo/) under accession number GSE36309.

Address correspondence and reprint requests to Prof. Qingqing Wang, 866 Yu Hang Tang Road, Institute of Immunology, Zhejiang University School of Medicine, Hangzhou 310058, People's Republic of China. E-mail address: wqq@zju.edu.cn

The online version of this article contains supplemental material.

Abbreviations used in this article: ARG1, arginase 1; MDSC, myeloid-derived suppressor cell; miR-494, microRNA-494; miRNA, microRNA; PTEN, phosphatase and tensin homolog; qRT-PCR, quantitative RT-PCR; SDF-1, stromal cell-derived factor; TCCM, tumor cell-conditioned medium; TDF, tumor-derived factor; 3′-UTR, 3′-untranslated region.

www.jimmunol.org/cgi/doi/10.4049/jimmunol.1103505

MicroRNAs (miRNAs), an abundant class of endogenous, small, noncoding RNAs of ~22 nucleotides in length, are post-transcriptional regulators that bind to specific cognate sequences in the 3′-untranslated region (3′-UTR) of target transcripts, usually resulting in translational repression and gene silencing. Mounting studies in recent years showed that miRNAs play crucial roles in the regulation of diverse biological processes, such as development, inflammation, and tumorigenesis (13). Our previous studies have shown that miRNAs participate in the regulation of macrophage function in inflammatory immune response (14, 15). However, it is still not clear whether and how miRNAs are involved in the regulation of MDSC biology.

In the current study, we investigated the possible involvement of miRNAs in governing the expansion and functions of MDSCs. We found that at high levels, microRNA-494 (miR-494) plays a critical role in regulating the nonimmunological activity of MDSCs in promotion of tumor progression. miR-494 activates the PI3K/Akt pathway by targeting of phosphatase and tensin homolog (PTEN) and hence not only enhances the ability of MDSCs to infiltrate into tumor tissue but also facilitates tumor invasion and metastasis via the upregulation of MMPs. These findings might provide new insights into the molecular mechanisms that regulate the expansion and functions of tumor-associated MDSCs and the exploration of potential targets for therapeutic intervention.

Materials and Methods

Animals, cell lines, and reagents

C57BL/6 and BALB/c mice (female, 6 to 8 wk old) were purchased from Shanghai Slac Animal (Shanghai, China). *Smad 3*-deficient mice established as previously described (16) were maintained under a specific pathogen-free condition. Experiments and animal care were performed according to protocols approved by the Zhejiang University Institutional Animal Care and Use Committee.

The 293FT cell line for generation of high-titer lentivirus was obtained from Invitrogen. The murine breast cancer 4T1 cells were a kind gift from Prof. Yangxin Fu (University of Chicago, Chicago, IL). Murine Lewis lung carcinoma (3LL), melanoma (B16), T lymphoma (EG7), B lymphoma (A20), and colon carcinoma (CT26) were obtained from American Type Culture Collection. Mice were injected s.c. in the flank (or the mammary fat pad for the 4T1 model) with 1×10^5 tumor cells. Three weeks later, tumor-bearing animals were used for the indicated studies.

DMSO, 6-thioguanine, GM6001, LY294002, rapamycin, and BAY-117082 were obtained from Sigma-Aldrich. Recombinant murine TGF-β1, GM-CSF, and IL-6 were purchased from R&D Systems. To generate tumor cell-conditioned medium (TCCM), subconfluent 4T1 tumor cells were kept in RPMI 1640 medium with a reduced (2%) serum concentration for 48 h. After that time, supernatants were collected, aliquoted, and kept at −80˚C until further use.

Isolation of the cells

A single-cell suspension was prepared from the spleen, bone marrow, and tumor tissue of the mice bearing 4T1, B16, EG7, A20, CT26 tumors. The cells were then subjected to 40%/70% Percoll (Sigma-Aldrich) gradient, and leukocytes were recovered from the interphase. Erythrocyte-depleted lymphocytes were isolated using anti–Gr-1 (clone RB6-8C5) conjugated to biotin followed by anti-biotin MicroBeads for Gr-1$^+$ cells. The purity of the cell population was >95%. CD11b$^+$Ly6G^{high}Ly6C^{low} granulocytic and CD11b$^+$Ly6G^{low}Ly6C^{high} monocytic MDSCs were isolated by cell sorting on a FACSAria II cell sorter (BD Biosciences). The purity of the cell populations was >99%.

Microarray assay

The miRNA microarray assay was conducted by service provider KangChen Bio-tech (Shanghai, China). Total RNA was harvested using TRIzol (Invitrogen) and the RNeasy Mini Kit (Qiagen), and the samples were then labeled using the miRCURY Hy3/Hy5 Power labeling kit and hybridized on the miRCURY LNA Array (v.11.0). Scanning was performed with the Axon GenePix 4000B microarray scanner. GenePix Pro V6.0 was used to read the raw intensity of the image. The intensity of green signal was calculated after background subtraction, and replicated spots on the same slide were averaged by getting a median intensity. We used the median normalization method to obtain "normalized data": normalized data = (foreground − background)/median; the median represents the 50% quantile of miRNA intensity which is >50 in all samples after background correction. Significance of results was determined via fold change and *t* test. The threshold value we used to screen differentially expressed miRNAs was fold change ≥1.30 or fold change ≤0.77 and p value <0.05. The microarray data were submitted to the Gene Expression Omnibus database (http://www.ncbi.nlm.nih.gov/geo/) under accession number GSE36309.

RNA isolation and real-time quantitative PCR

Real-time quantitative RT-PCR (qRT-PCR) analysis was performed using an ABI 7500 system (Applied Biosystems) and SYBR RT-PCR kits (Takara). The relative expression level of miRNAs was normalized to that of internal control U6 by using the $2^{-\Delta\Delta Ct}$ cycle threshold method. The primers for detecting all the miRNAs are described in Supplemental Table I. For ARG1, MMP2, MMP9, MMP13, MMP14, and PTEN mRNA analysis, the primers are also listed in Supplemental Table I. Data were normalized by the level of GAPDH expression.

Flow cytometry

Flow cytometry was conducted using a BD Biosciences LSR device and analyzed with FlowJo (Tree Star). Phospho-Akt staining was carried out using the Cytofix/Cytoperm kit (BD Biosciences). Abs used for FACS staining were anti-mouse Gr-1, CD11b, Ly6G, Ly6C, and Annexin V Apoptosis Detection Kit from BD Biosciences, anti-CXCR4 from BioLegend, and anti–p-Akt from Cell Signaling Technology.

Lentiviral vector construction

A genomic sequence spanning the mouse miR-494 coding region flanked by ~100 bp from 5′ or 3′ on either end, a sequence encoding scrambled oligonucleotide control, or miR-494 specific inhibitor (sponge) was cloned into the pSIF-H1-coGFP Lentivector (System Biosciences). For overexpression of PTEN, a sequence encoding the CDS region of *PTEN* was cloned into the pCDF1-MCS2-EF1-copGFP Vector (System Biosciences).

In vitro cell migration and invasion assays

To assess cell migration, MDSCs were seeded onto the top chamber of Transwell filters (8 μm; Costar). The filters were placed in a 24-well plate containing medium with recombinant murine stromal cell-derived factor-1 (SDF-1/CXCL12) at 100 ng/ml. Migrated MDSCs were counted (five fields/well) 6–8 h after incubation. For in vitro invasion assay, 4T1 cells were labeled with CMTMR (Molecular Probes), after which 4T1 cells with or without MDSCs (labeled with CFSE) were seeded onto the top chamber of Transwell filters coated with Matrigel (Becton-Dickinson). The filters were placed in a 24-well plate containing culture media of 10% FCS. Invaded 4T1 cells were counted (five fields/filter) 6–8 h after incubation.

In vivo miR-494 manipulation experiment

4T1 cells (1×10^5) were injected into the mammary fat pad of female BALB/c mice. Then, 2.5×10^7 PFU lentivirus containing miR-494 specific inhibitor (lv-sponge) or scrambled oligonucleotide control (lv-ctrl) was i.v. administered, and the 2.43 mAb or the isotype was given to the mice i.p. (100 μg/mouse) on days 3, 10, and 17 after tumor inoculations. Tumor measurements were performed with a caliper by measuring the largest diameter and its perpendicular length; the tumor size index is the average of the product of these diameters. Primary tumors were surgically resected on day 24. Five mice in each group were sacrificed for the analysis of lung metastases with the colonogenic assay. Five mice in each group were observed for survival >50 d postsurgery. Immunostaining of MDSCs in tumor tissue was performed using biotinylated anti–Gr-1 (eBioscience), followed by PE-conjugated streptavidin (eBioscience). Slides were viewed with an Olympus IX71 fluorescent microscopy (Olympus) using an LUCPlanFLN lens at ×40/NA 0.6. Images were acquired using a DP2 digital camera and were processed with DP2-BSW and Adobe Photoshop version 8.0 software (Adobe Systems).

Colonogenic assay

Lungs were collected and chopped before being dissociated in DMEM supplemented with 10% FCS containing 1.5 mg/ml collagenase type D (Sigma-Aldrich) for 30 min in a 37˚C incubator with shaking at 178 rpm. Organs were plated at various dilutions in the DMEM supplemented with 10% FCS and 60 μM 6-thioguanine. Individual colonies representing micrometastasis were counted after 5–10 d as previously described (17).

3′-UTR luciferase reporter assays

The *PTEN* 3′-UTR luciferase reporter construct was made by amplifying the mouse *PTEN* mRNA 3′-UTR sequence and cloning it downstream of the CMV-driven firefly luciferase cassette in the pMIR-REPORT vector (Ambion). HEK-293 cells were cotransfected with 80 ng luciferase reporter plasmid, 40 ng pRL-TK-Renilla-luciferase plasmid, and the indicated RNAs (final concentration, 20 nM). Luciferase activities were measured using the Dual-Luciferase Reporter Assay System (Promega).

Western blot analysis

Lysates from purified cells were denatured and subjected to SDS-PAGE; proteins were transferred to polyvinylidene difluoride membranes. The membranes were incubated with the primary Abs against PTEN, Akt, mTOR, NF-κB, β-actin and phosphorylated Akt, mTOR, NF-κB p65, followed by hybridization with the secondary HRP-conjugated Abs. Detection was performed as described previously (18).

Statistical analysis

Statistical analysis was performed using Student *t* test, ANOVA, and log-rank test (for survival analysis) using SPSS (version 10.0), with a p value <0.05 considered statistically significant.

Results

miR-494 is highly expressed in tumor-expanded MDSCs

By comparing the miRNA expression profile between Gr-1$^+$ CD11b$^+$ cells from 4T1-bearing mice (MDSCs) and their counterpart from tumor-free mice using an array-based miRNA profiling, eight differentially expressed miRNAs were identified. Three were upregulated (miR-494, miR-882, miR-361) and five were downregulated (miR-466j, let-7e, miR-133b, miR-713, miR-322) (Fig. 1A). We confirmed the expression of these miRNAs by qRT-PCR analysis (Fig. 1B). Consistent with the array data, the result showed that miR-494 had the highest expression and the most significant difference (tumor versus control, $p < 0.01$). MDSCs consist of two major subsets of CD11b$^+$Ly6G^{high}Ly6C^{low} granulocytic and CD11b$^+$Ly6G^{low}Ly6C^{high} monocytic cells. We further detected the expression of miR-494 in both mononuclear and polymorphonuclear MDSCs isolated from the bone marrow of 4T1-bearing mice by cell sorting. As shown in Fig. 1C, significantly increased expression of miR-494 was detected in both subpopulations compared with their counterpart from tumor-free mice (granulocytic MDSCs, $p < 0.01$; monocytic MDSCs, $p < 0.001$).

To address whether our observation that miR-494 upregulation in 4T1 tumor-expanded MDSCs could be extrapolated to MDSCs expanded by other tumors, 3LL Lewis lung carcinoma, B16 melanoma, EG7 T lymphoma, A20 lymphoma, and CT26 colon carcinoma were established by injecting 1×10^5 cells s.c. into the mice. A significant increase in the proportion of Gr-1$^+$ CD11b$^+$ MDSCs in the spleens was observed in all tumor models (Supplemental Fig. 1, tumor versus control, all $p < 0.01$). Importantly, significant upregulation of miR-494 was observed in MDSCs derived from all these tumors, although there was variation between different models (Fig. 1D). These results indicated that the upregulation of miR-494 is the common intrinsic character of MDSCs in these established tumor models.

Tumor-derived factors, especially TGF-β1, markedly induce the upregulation of miR-494 in MDSCs

Previous studies have demonstrated that the expansion and acquisition of immunosuppressive activity of MDSCs in vivo and in vitro can be mediated by tumor-derived factors (TDFs) (12, 19, 20). Gr-1$^+$ CD11b$^+$ cells isolated from tumor-free mice do not show a relevant suppressive activity and quickly differentiate into mature granulocytes, macrophages, or dendritic cells. However, Gr-1$^+$ CD11b$^+$ cells isolated from tumor-bearing mice have immunosuppressive activity and impaired ability to differentiate into mature cells (4). Moreover, compared with MDSCs isolated from lymphoid organs or peripheral blood, tumor-infiltrating MDSCs show a stronger ability to suppress adaptive immune response and facilitate tumor cell invasion and metastasis via release of various MMPs (21, 22). To investigate whether miR-494 expression is also regulated by TDFs, Gr-1$^+$ CD11b$^+$ cells isolated from tumor-free mice were cultured with 4T1 TCCM. As expected, we found that miR-494 expression was significantly induced by TCCM in a dose-dependent manner (Fig. 2A).

Some TDFs have been reported to induce MDSC expansion, including IL-6 and GM-CSF (23). As shown in Fig. 2B, we found that the expression of miR-494 in Gr-1$^+$ CD11b$^+$ cells was not affected by GM-CSF and IL-6, but interestingly, miR-494 expression was significantly induced by TGF-β1 treatment ($p < 0.001$). Moreover, the induction of miR-494 was partially blocked by anti–TGF-β1 mAb in cells stimulated with 4T1 TCCM (Fig. 2C), and the upregulation of miR-494 was impaired in Smad 3-deficient Gr-1$^+$ CD11b$^+$ cells isolated from the spleen of Smad $3^{-/-}$ mice (Fig. 2D). Therefore, it suggested that TGF-β1 is an important factor responsible for the miR-494 upregulation in MDSCs and it induces the expression of miR-494 via the Smad 3-dependent pathway. Because blockade of TGF-β1 by anti–TGF-β1 mAb or cells from Smad $3^{-/-}$ mice could not completely block the effect of TCCM, it indicated that the induction of miR-494 may be the combined effect of several cytokines.

More interestingly, the expression of ARG1, MMP2, MMP13, and MMP14 in MDSCs was closely correlated to the expression level of miR-494 at the indicated time points upon TCCM stimulation, whereas the expression of MMP9 did not show a significant change (Supplemental Fig. 2). We observed a similar increase in the expression of ARG1, MMP2, MMP13, and MMP14 in Gr-1$^+$ CD11b$^+$ cells stimulated with TGF-β1 (Fig. 2E).

Given that tumor-infiltrating MDSCs possess a stronger ability to promote tumor progression compared with MDSCs isolated from lymphoid organs, we compared the expressions of miR-494 and MMPs in MDSCs isolated from the spleens (sp-MDSC) and tumor tissues (tu-MDSC). A 10-fold increase in the level of miR-494 was accompanied by dramatically high expression levels of ARG1, MMP2, MMP13, and MMP14 in tu-MDSC compared with sp-MDSC from 4T1-bearing mice (Fig. 3). Taken together, these data suggested that the expression level of miR-494 might be involved in the activation and functions of MDSCs.

The migration and functions of tumor-expanded MDSCs are miR-494 dependent

To investigate further the role of miR-494 in regulating the activity of MDSCs, we constructed lentiviral vectors containing mir-494 (lv-494), its specific inhibitor (lv-sponge), and scrambled oligonucleotide control (lv-ctrl) for miR-494 manipulation. The transfection efficiency of lentiviral vectors was >80% in the whole MDSC cell population even at a very low multiplicity of infection (Supplemental Fig. 3A), and a significantly high level of miR-494 expression was demonstrated in cells after lv-494 transfection by qRT-PCR (Supplemental Fig. 3B), which suggested lentiviral vectors were suitable for miR-494 manipulation.

First, we determined whether the manipulation of miR-494 could influence the viability of MDSCs. 4T1-expanded MDSCs were infected with lv-494, lv-sponge, or lv-ctrl, and there was no difference in the proportion of apoptotic cells at the 24-h time point regardless of overexpression or knockdown of miR-494 (data not shown). Notably, a dramatic decrease in the proportion of annexin V-positive cells was observed in lv-494–infected MDSCs compared with lv-ctrl MDSCs at the 72-h time point ($p < 0.01$), whereas lv-

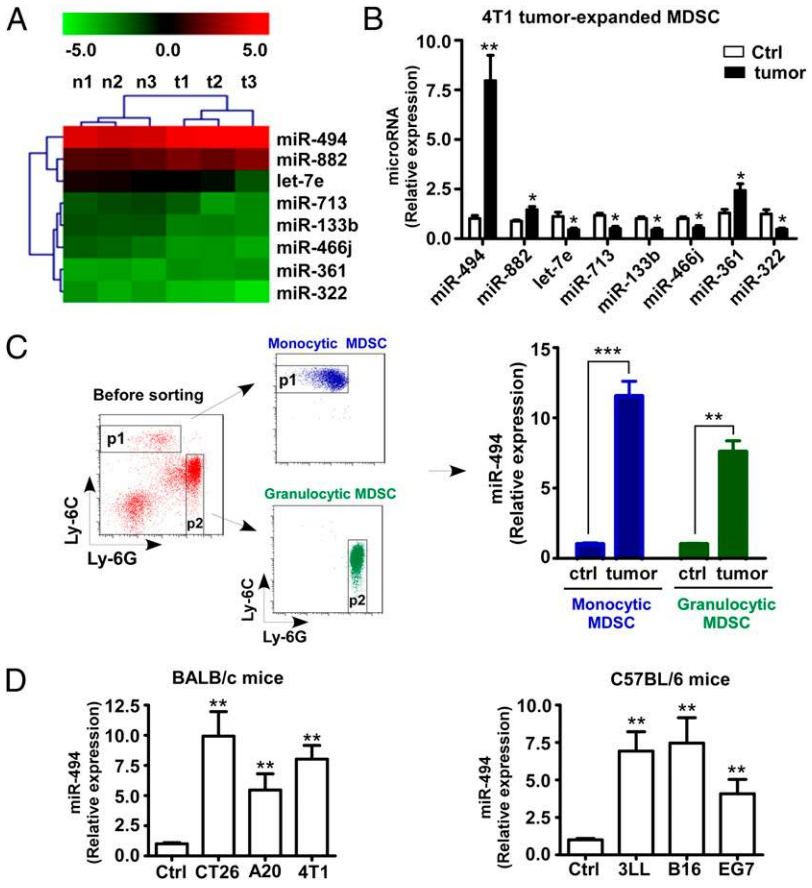

FIGURE 1. Upregulation of miR-494 in Gr-1$^+$ CD11b$^+$ cells from the tumor-bearing mice compared with those from tumor-free mice. (**A**) Gr-1$^+$ CD11b$^+$ cells were isolated by immunomagnetic selection from the bone marrow of 4T1 tumor-bearing mice 3 wk after tumor inoculation (n = 3) and of tumor-free BALB/c mice (n = 3), then the miRNA expression profiles were analyzed using miRCURY LNA microRNA Arrays. The heat map diagram shows the result of the two-way hierarchical clustering of genes and samples, and the clustering was performed on the differentially expressed miRNAs (only differentially expressed miRNAs with fold change ≥1.30 or fold change ≤0.77 and p value <0.05 are included). The color scale shown at the top illustrates the relative expression level of an miRNA: red represents a high expression level; green represents a low expression level. (**B**) The expression levels of these miRNAs were measured by qRT-PCR and normalized to the expression of U6 in each sample. Data are the mean ± SD (n = 4) of one representative experiment. Similar results were obtained in three independent experiments. (**C**) CD11b$^+$Ly6G^{high}Ly6C^{low} granulocytic and CD11b$^+$Ly6G^{low}Ly6C^{high} monocytic MDSCs were isolated from the bone marrow of 4T1 tumor-bearing mice 3 wk after tumor inoculation and of tumor-free mice by cell sorting. miR-494 expression in both subsets was measured by qRT-PCR. Data are the mean ± SD (n = 4) of one representative experiment. Similar results were obtained in three independent experiments. (**D**) miR-494 expression in Gr-1$^+$ CD11b$^+$ cells isolated from the bone marrow of mice with different tumors was measured by qRT-PCR. Data are the mean ± SD (n = 4) of one representative experiment out of three performed. *$p < 0.05$, **$p < 0.01$, ***$p < 0.001$.

sponge markedly induced the apoptosis of MDSCs (Fig. 4A, lv-sponge versus lv-ctrl, $p < 0.01$). It indicated that the prolonged life span of MDSCs by miR-494 may partially contribute to the expansion and accumulation of MDSCs in tumor-bearing mice.

We then detected whether the manipulation of miR-494 could affect the expression of ARG1 and MMPs in MDSCs. As expected, the expression levels of ARG1, MMP2, MMP13, and MMP14 were significantly upregulated in lv-494–infected MDSCs compared with those in lv-ctrl–infected MDSCs (Fig. 4B); moreover, lv-sponge overtly blocked the induction in the expression of these molecules. To confirm further the effects of miR-494–induced MMPs in MDSCs on tumor invasion, we performed in vitro invasion assays. 4T1 cells labeled with CMTMR alone or with lv-494–infected MDSCs labeled with CFSE were seeded into the top chamber of Transwell filters coated with Matrigel. We found a significant increase in 4T1 cell invasion when they were mixed with lv-494–infected MDSCs. Importantly, GM6001, an inhibitor of MMPs, dramatically attenuated the cell invasion (Fig. 4C, 4D). These data strongly indicated that miR-494 plays a key role in regulating the nonimmunological functions of MDSCs for the facilitation of tumor cell invasion.

Next, we tried to investigate whether miR-494 also regulates the migration of MDSCs. It has been previously reported that the chemokine receptor axis SDF-1/CXCR4 serves as an intrinsic mechanism for the recruitment of MDSCs into tumors (11). We examined the expression of CXCR4 on the surface of MDSCs and found no significant difference regardless of overexpression or inhibition of miR-494 in MDSCs (Fig. 4E). Notably, the in vitro cell migration assays showed that miR-494 indeed increased the efficiency of CXCR4-mediated chemotaxis, whereas miR-494 sponge markedly inhibited the migration of MDSCs (Fig. 4F).

In addition, we tested whether the expression of miR-494 could influence the immunosuppressive activity of MDSCs. The EG7 tumor model was used to investigate the possible role of miR-494 in regulating the Ag-specific T cell hyporesponsiveness induced by MDSCs. MDSCs isolated from EG7-bearing mice were infected with the indicated lentiviral vectors. As shown in Fig. 4G, OT-1 CD8$^+$ T cell proliferation was significantly suppressed by lv-494–infected MDSCs in comparison with lv-ctrl–infected MDSCs, and this suppressive activity could be partially blocked by an ARG1 inhibitor nor-NOHA. Infection of MDSCs with lv-sponge had very limited effect on OT-1 cell proliferation.

Taken together, the data suggested that high level of miR-494 in MDSCs not only altered the intrinsic apoptotic/survival signal but also enhanced the efficiency of CXCR4-mediated chemotaxis, the immunosuppressive activity, and the ability to facilitate tumor cell invasion, thus indicating that the activity of tumor-expanded MDSCs is miR-494 dependent.

Knockdown of miR-494 attenuates primary tumor growth and metastasis in vivo

To investigate whether the manipulation of miR-494 in MDSCs could influence the tumor progress in vivo, we used a spontaneously metastasizing 4T1 mammary tumor model that closely mimics human breast cancer. We also observed the effect of lv-sponge on tumor metastasis in a CD8$^+$ T cell depletion group to exclude the influence of primary tumor size on lung metastasis. The mechanism of miR-494 sponge is specifically to block the interaction of miR-494 with its real targets via competitive binding of miR-494. First, we detected the expression of mir-494 in various types of cells and lymphoid organs by RT-PCR. mir-494 expression was barely detected in 4T1 tumor cells or T or

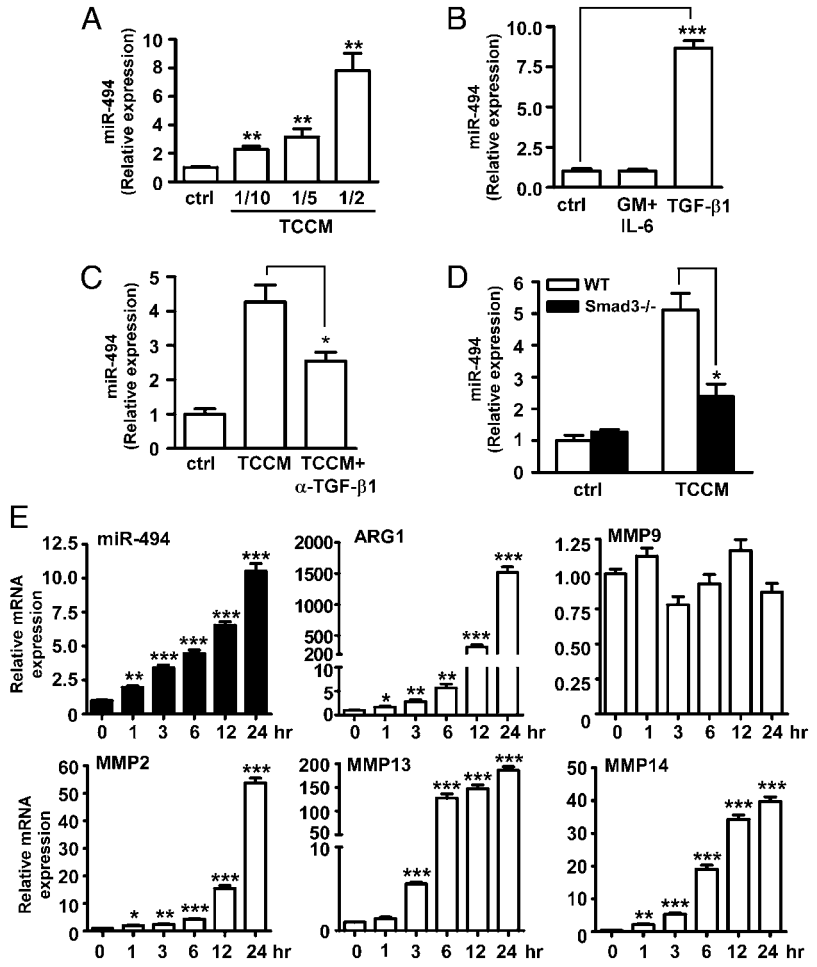

FIGURE 2. TGF-β1 is responsible for the upregulation of miR-494 in MDSCs. Gr-1$^+$ CD11b$^+$ cells isolated from the bone marrow of naive mice were cultured with fresh medium (ctrl) with serial dilution of TCCM (**A**) or fresh medium (ctrl) with 10 ng/ml TGF-β1, 10 ng/ml GM-CSF plus 10 ng/ml IL-6 (**B**), or 10 μg/ml anti–TGF-β1 Ab (**C**). The expression of miR-494 was examined by qRT-PCR 24 h later. (**D**) Gr-1$^+$ CD11b$^+$ cells isolated from the bone marrow of *Smad 3*-deficient mice were cultured with or without TCCM for 24 h. (**E**) Gr-1$^+$ CD11b$^+$ cells from tumor-free BALB/c mice were cultured with 10 ng/ml TGF-β1 for the indicated time points, and the mRNA expression of miR-494, ARG1, MMP2, MMP13, and MMP14 was measured by qRT-PCR. Data are the mean ± SD (n = 4) of one representative experiment. Similar results were obtained in three independent experiments. *$p < 0.05$, **$p < 0.01$, ***$p < 0.001$.

B lymphocytes, so it can be expected that administration of lv-sponge mainly inhibits the function of highly expressed miR-494 in MDSCs (Supplemental Fig. 3C). As shown in Fig. 5A and 5B, the growth of the primary tumors was significantly reduced and colonies of metastatic cells were rarely detected in the lungs of mice treated with lv-sponge, whereas a high number of lung metastases was detected in the mice treated with lv-ctrl (lv-sponge + iso mAb group versus lv-ctrl + iso mAb group, $p < 0.01$). The inhibitory effect of lv-sponge on primary tumor growth is most likely due to the enhanced CTL activity resulting from the reduction of MDSC accumulation in tumor tissue, because the depletion of CD8$^+$ T cells restored the primary tumor growth (Fig. 5A). More importantly, depletion of CD8$^+$ T cells barely affected the anti-metastatic effect of lv-sponge (lv-sponge + 2.43 mAb group versus lv-sponge + iso mAb group, $p > 0.05$) (Fig. 5B). Impressively, although CD8$^+$ T cell depletion (lv-sponge + 2.43 mAb group) restored the primary tumor growth and the accumulation of MDSCs in the spleen (compared with the lv-sponge + iso mAb

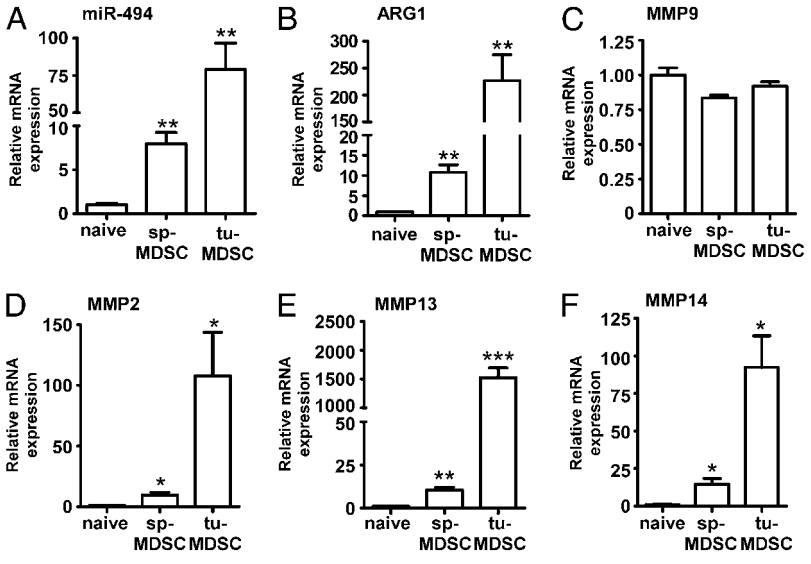

FIGURE 3. Different expression levels of miR-494, ARG1, and MMPs in the splenic MDSCs and tumor-infiltrating MDSCs. Gr-1$^+$ CD11b$^+$ cells were isolated from naive BALB/c mice (naive), the spleen of 4T1 tumor-bearing mice (sp-MDSC), and 4T1 tumor tissues (tu-MDSC) 3 wk after tumor inoculation. The mRNA expression of miR-494 (**A**), ARG1 (**B**), MMP9 (**C**), MMP2 (**D**), MMP13 (**E**), and MMP14 (**F**) was measured by qRT-PCR. Data are the mean ± SD (n = 4) of one representative experiment. Similar results were obtained in three independent experiments. *$p < 0.05$, **$p < 0.01$, ***$p < 0.001$.

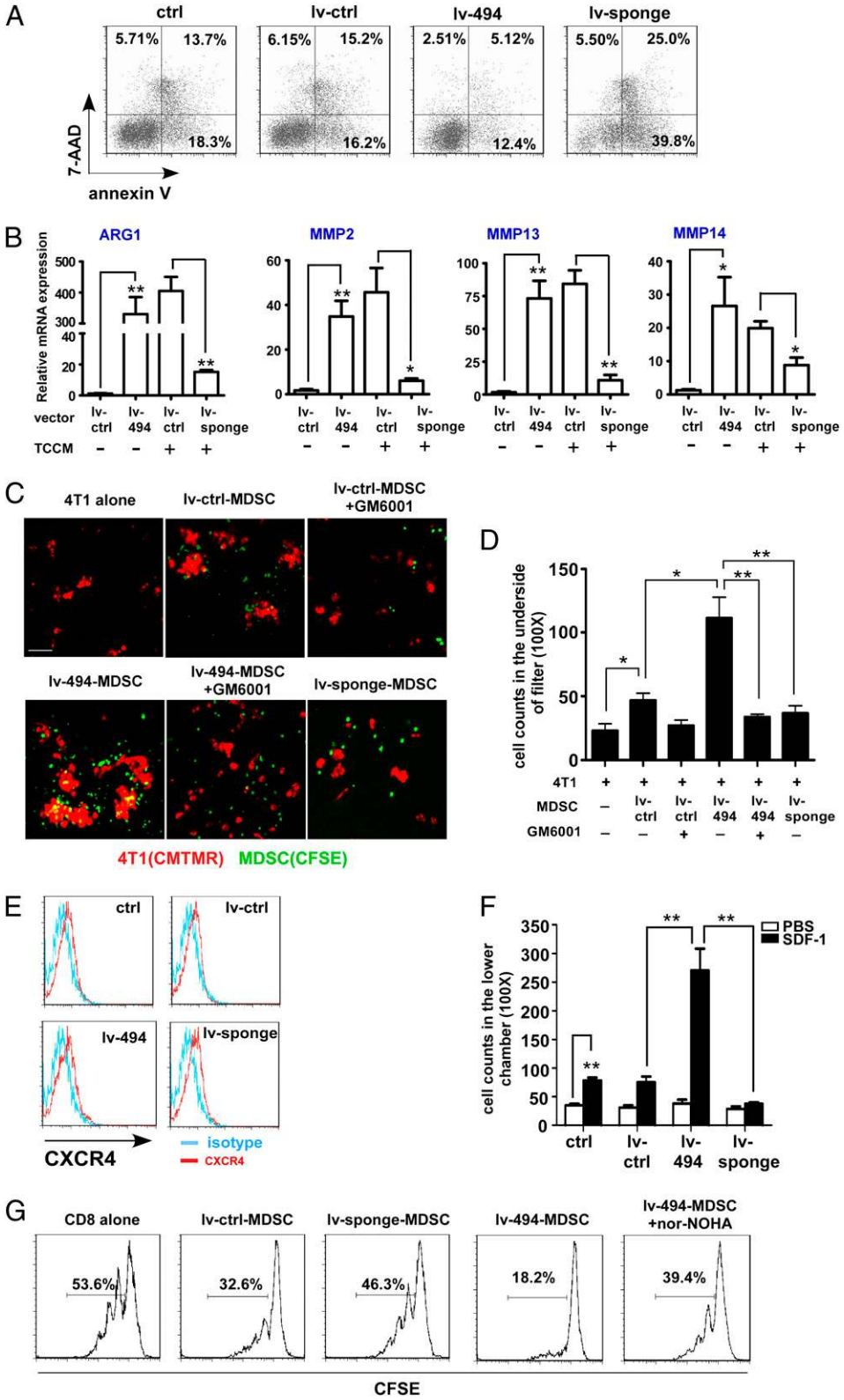

FIGURE 4. The migration and functions of tumor-expanded MDSCs are miR-494 dependent. (**A**) 4T1 tumor-expanded Gr-1$^+$ CD11b$^+$ MDSCs isolated 3 wk after tumor inoculation were infected with the indicated lentivirus, cultured for 3 d, and stained with annexin V–allophycocyanin and 7-amino-actinomycin D (7-AAD) for flow cytometry analysis of apoptosis. One representative experiment out of three is shown. (**B**) 4T1-expanded MDSCs were infected overnight with lentivirus containing mir-494 (lv-494), its specific inhibitor (lv-sponge), and scrambled oligonucleotide control (lv-ctrl) for miR-494 manipulation, then cultured with or without 4T1 TCCM for 24 h. The expression of ARG1, MMP2, MMP13, and MMP14 was determined by qRT-PCR. Data are the mean ± SD ($n = 4$) of one representative experiment. Similar results were obtained in three independent experiments. (**C**) Representative images of invaded 4T1 cells. MDSCs were infected with the indicated lentivirus overnight and labeled with CFSE (green). CMTMR-labeled (red) 4T1 cells with or without MDSCs were seeded into the top chamber of Transwell filters. After 6–8 h, invaded 4T1 cells were counted (five fields/filter). GM-6001 (1 μM), an inhibitor of MMPs, was used to determine the effect of MMPs on cell invasion. Scale bar, 50 μm. (**D**) The quantitative data for the 4T1 cell invasion. Shown is one representative experiment of three performed. (**E**) MDSCs were infected with lv-494, lv-sponge, or lv-ctrl and stained with *(Figure legend continues)*

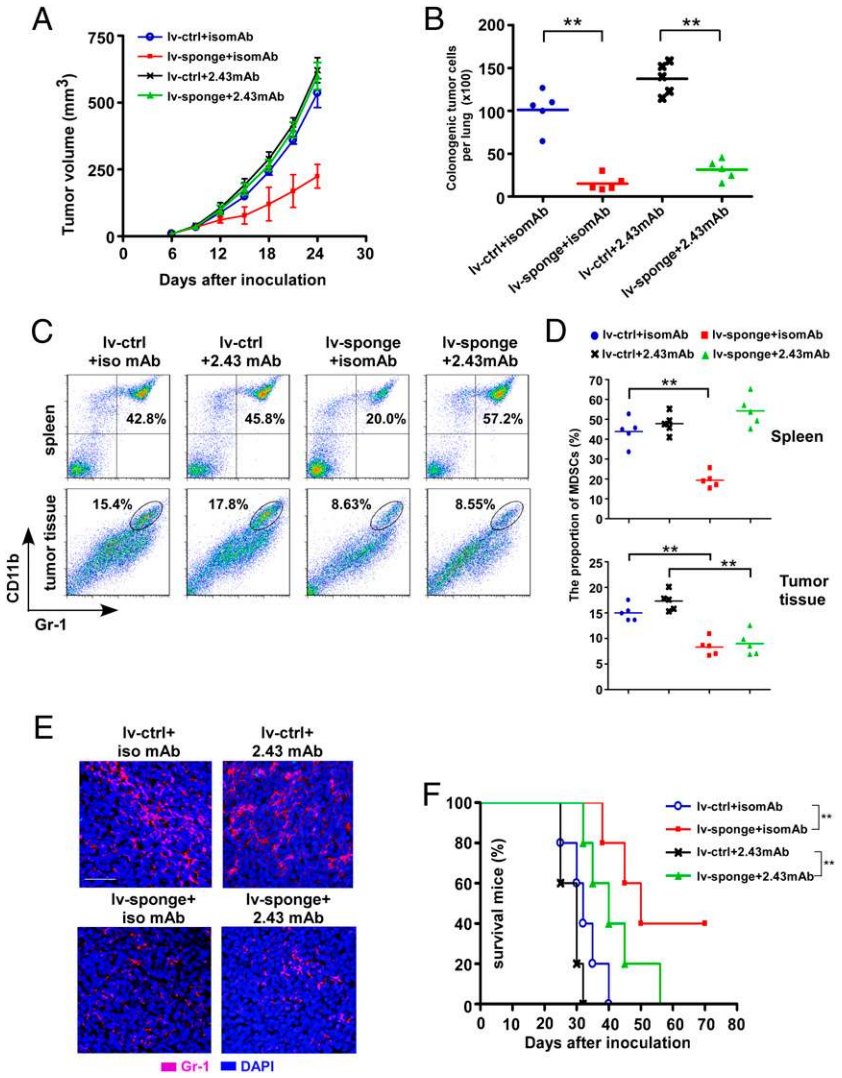

FIGURE 5. Knockdown of miR-494 expression attenuated tumor growth and metastasis in vivo. 4T1 tumor cells (1×10^5) were injected into the mammary fat pads of female BALB/c mice (n = 10). Then, 2.5×10^7 PFU lv-sponge or lv-ctrl was i.v. administered, and the 2.43 mAb or the isotype control was given to mice, 100 μg/mouse i.p., on days 3, 10, and 17 after tumor inoculation. (**A**) Primary tumor growth in the indicated different groups was monitored. Twenty-four days after tumor inoculation, five mice in each group were sacrificed. (**B**) Lung metastases were determined by the colonogenic assay as described in *Materials and Methods*. Data are the mean ± SD (n = 5) of one representative experiment. Similar results were obtained in at least three independent experiments. (**C**) The proportion of Gr-1$^+$ CD11b$^+$ MDSCs in the spleen and tumor tissues was analyzed by flow cytometry. Shown is one representative experiment. (**D**) The proportion of Gr-1$^+$ CD11b$^+$ MDSCs in the spleen and tumor tissues. Data are the mean ± SD (n = 5) of one representative experiment. Similar results were obtained in at least three independent experiments. (**E**) MDSC accumulation in the tumor tissues was also analyzed by immunofluorescent staining with PE-labeled anti–Gr-1 mAb. Scale bar, 50 μm. (**F**) Primary tumors were surgically resected 24 d after inoculation, and five mice in each group were monitored for survival. $^{**}p < 0.01$.

group, $p < 0.01$), the number of tumor-infiltrating MDSCs in the lv-sponge + 2.43 mAb group still exhibited a dramatic decrease compared with that in mice treated with lv-ctrl + 2.43 mAb ($p < 0.01$) (Fig. 5C–E). It indicated that knockdown of miR-494 indeed impaired the ability of MDSCs to infiltrate into the tumor tissue. These results suggested that knockdown of miR-494 not only inhibited the primary tumor growth by the increased CD8$^+$ T cell response, which resulted from the decreased MDSC accumulation in the tumor sites, but also impaired the intrinsic ability of MDSCs to facilitate tumor invasion and metastasis.

Furthermore, the combination therapy of lv-sponge and surgery significantly prolonged the survival period of tumor-bearing mice, 40% of which survived and remained healthy >50 d postsurgery, whereas all the mice in the lv-ctrl group died of metastases (lv-sponge + iso mAb group versus lv-ctrl + iso mAb group, $p < 0.01$, Fig. 5F). Therefore, miR-494 might be a potential target for therapeutic intervention of mammary carcinoma with metastatic properties.

PTEN is a functional target of miR-494, and the PTEN/Akt pathway is critical for the activation of MDSCs

It is generally accepted that miRNAs exert their function through regulating the expression of their target genes. Thus, we took advantage of multiple prediction algorithms (miRBase, PicTar, and TargetScan v.5.1) to identify the potential miR-494 targets related to the functions of tumor-associated MDSCs. Among hundreds of potential target genes, *PTEN*, a major negative regulator of the PI3K/Akt signaling pathway involved in cell growth, apoptosis, motility, and differentiation, was demonstrated in this study to be a functional target of miR-494 in MDSCs. It is known that PTEN plays an essential role in neutrophil spontaneous death and can negatively regulate CXCR4-mediated chemotaxis (24, 25). We first compared PTEN mRNA and protein expression levels between tumor-expanded MDSCs and Gr-1$^+$ CD11b$^+$ cells from tumor-free mice. Notably, the PTEN protein level was significantly downregulated in tumor-expanded MDSCs compared with that in Gr-1$^+$ CD11b$^+$ cells

anti-CXCR4–allophycocyanin for flow cytometry analysis. Shown is one representative experiment out of three. (**F**) MDSCs infected with the indicated lentivirus were incubated with SDF-1 (100 ng/ml) or PBS control. Cells that migrated were counted after 8 h (five fields/well). Similar results were obtained in three independent experiments. (**G**) Gr-1$^+$ CD11b$^+$ cells from the spleens of EG7 tumor-bearing mice were infected with the indicated lentivirus overnight and cocultured with CFSE-labeled OT-1 CD8$^+$ T cells (1:3 ratio) loaded with SIINFEKL (10 μg/ml) with or without nor-NOHA (0.5 mM), an ARG1 inhibitor. The proliferation of CD8$^+$ T cells was evaluated 3 d later with CFSE dilution by flow cytometry. One representative experiment of three performed is shown. $^*p < 0.05$, $^{**}p < 0.01$.

from tumor-free mice, whereas PTEN mRNA expression showed no difference (Fig. 6A). The inconsistency between PTEN mRNA and protein levels hints that an miRNA-mediated mechanism may be involved. To confirm further the possibility that PTEN may be regulated posttranscriptionally by miR-494, 3′-UTR of PTEN reporter plasmid was constructed. When the reporter plasmids with miR-494 mimics or the scrambled oligonucleotide were cotransfected to HEK-293 cells, we observed that the miR-494 mimics markedly decreased the luciferase activity (Fig. 6B). Furthermore, transfection of lv-494 significantly decreased PTEN expression in MDSCs, thus suggesting that endogenous PTEN is targeted and regulated by miR-494 (Fig. 6C).

To confirm whether miR-494–induced activation of MDSCs was mediated by targeting of PTEN expression, we designed a lentiviral vector encoding 3′-UTR–depleted *PTEN* to enforce the expression of PTEN in MDSCs. Overexpression of PTEN in Gr-1$^+$ CD11b$^+$ cells did not affect the TDF-induced miR-494 upregulation, whereas the increased expression of MMPs induced by TCCM were significantly blocked (Fig. 6D), and SDF-1/CXCL12-mediated MDSC migration was abrogated (Fig. 6E). These data

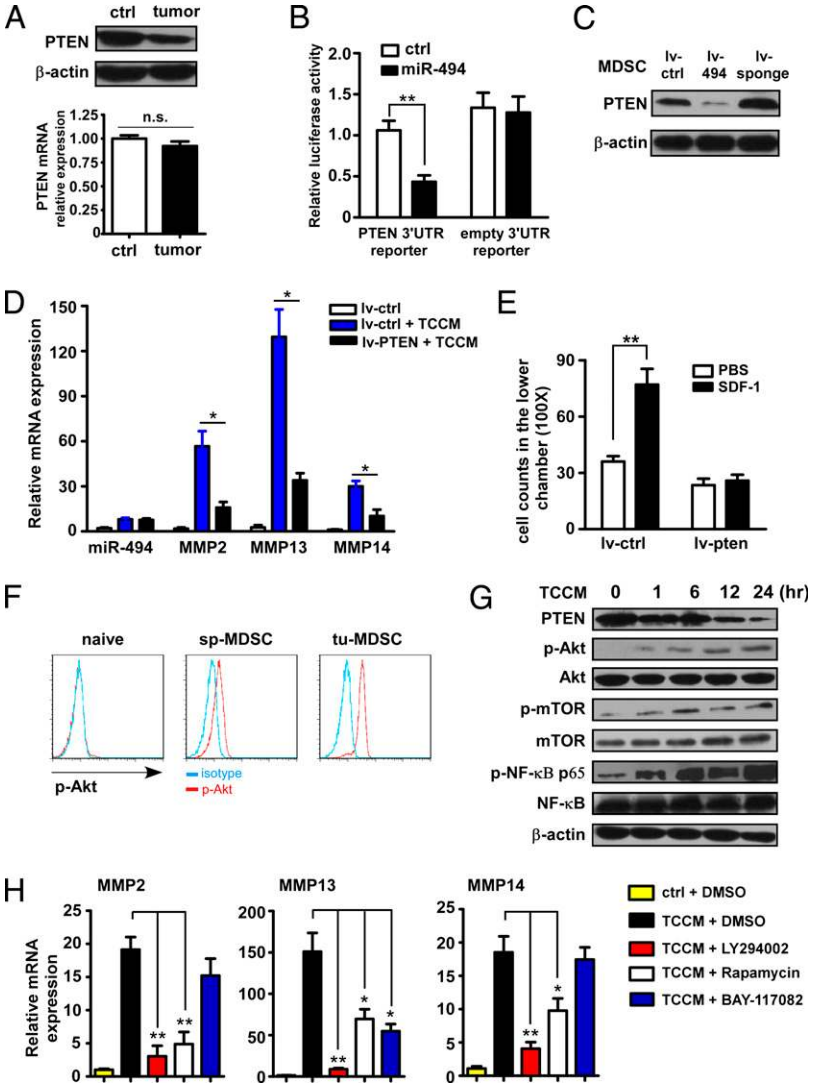

FIGURE 6. PTEN is a functional target of miR-494 and is essential for the activation of MDSCs. (**A**) Gr-1$^+$ CD11b$^+$ cells were isolated from the bone marrow of naive BALB/c (ctrl) and 4T1-bearing (tumor) mice 3 wk after tumor inoculation. PTEN mRNA and protein levels were detected by qRT-PCR and Western blot. Data are the mean ± SD ($n = 4$) of one representative experiment. Similar results were obtained in at least three independent experiments. (**B**) HEK-293 cells were cotransfected with miR-494 mimics (20 nM) or the matched control, 80 ng of indicated vectors, and 40 ng of pRL-TK. After 24 h, firefly luciferase activity was measured and normalized by Renilla luciferase activity. Data are the mean ± SD ($n = 4$) of one representative experiment. Similar results were obtained in at least three independent experiments. (**C**) 4T1-expanded Gr-1$^+$ CD11b$^+$ cells were infected with the indicated lentivirus for 24 h, and PTEN levels were detected by immunoblot analysis. Shown is one representative experiment out of three. (**D**) Gr-1$^+$ CD11b$^+$ cells from the bone marrow of naive BALB/c mice were infected with lv-PTEN and cultured with 4T1 TCCM. Expression levels of miR-494 and MMPs (MMP2, MMP13, MMP14) were examined by qRT-PCR. Data are the mean ± SD ($n = 4$) of one representative experiment. Similar results were obtained in at least three independent experiments. (**E**) 4T1-expanded Gr-1$^+$ CD11b$^+$ cells were infected with lv-PTEN and collected for the in vitro cell migration assay performed as described in *Materials and Methods*. Shown is one representative experiment of three performed. (**F**) Phosphorylation of Akt in Gr-1$^+$ CD11b$^+$ cells isolated from the spleen of naive BALB/c mice (naive), 4T1-bearing mice (sp-MDSC), and 4T1 tumor tissues (tu-MDSC) was measured by flow cytometry. The result of one representative experiment is shown. (**G**) Gr-1$^+$ CD11b$^+$ cells from naive BALB/c mice were cultured with 4T1 TCCM for the indicated time points. Cells were collected, and the protein expression of PTEN, p-Akt, p-mTOR, and p–NF-κB (p-p65) was detected by immunoblot. Shown is one representative experiment out of three. (**H**) The expression level of MMPs was examined by qRT-PCR in Gr-1$^+$ CD11b$^+$ cells from naive mice cultured with 4T1 TCCM and treated with the indicated inhibitors (50 μM LY294002; 10 μM BAY-117082; 10 nM rapamycin) for 24 h. Data are the mean ± SD ($n = 4$) of one representative experiment. Similar results were obtained in at least three independent experiments. $^*p < 0.05$, $^{**}p < 0.01$.

strongly indicated that the PTEN expression downregulated by miR-494 is essential for the activation of MDSCs.

Given that PTEN acts as a major negative regulator of the PI3K/Akt signaling pathway, the phosphorylation level of Akt in Gr-1$^+$ CD11b$^+$ cells from naive mice, 4T1-expanded splenic MDSCs, and tumor-infiltrating MDSCs was examined. As shown in Fig. 6F, a significantly high level of p-Akt was detected in tumor-expanded MDSCs compared with that in controls, indicating that the Akt pathway might be important for the activation of tumor-expanded MDSCs. Significantly reduced PTEN expression was also detected in Gr-1$^+$ CD11b$^+$ cells after TCCM stimulation (Fig. 6G); this was inversely correlated with the phosphorylation levels of mTOR and NF-κB. Previous studies have reported that the mTOR and NF-κB pathways are related to the expression of MMPs (26–28). To determine how these molecules were involved, Gr-1$^+$ CD11b$^+$ cells from naive mice were cultured with TCCM in the presence of LY294002, BAY-117082, or rapamycin, which were used to inhibit Akt, NF-κB, and mTOR, respectively. As shown in Fig. 6H, the increased levels of MMPs induced by TCCM were completely abolished by LY294002, suggesting that the Akt activity is indispensable for the activation of MDSCs. BAY-117802 significantly blocked MMP13 expression but had a limited effect on the upregulation of MMP2 and MMP14, whereas rapamycin eliminated the expression of all MMPs. These data indicated that the upregulation of miR-494 led to an inhibition of PTEN expression, thereby resulting in an increase in the Akt activity and the subsequent activation of NF-κB and mTOR, all of which played critical roles in controlling MDSC activity.

In conclusion, our findings suggested a new regulatory pathway controlling the activation of tumor-expanded MDSCs (working model, Fig. 7). TGF-β1–induced miR-494 was involved in the negative regulation of PTEN expression. Downregulation of PTEN enhanced the activity of Akt and its downstream pathways, promoted the accumulation of MDSCs in tumor tissues, and resulted in the induction of high levels of metalloproteinases (MMP2, MMP13, and MMP14), which are key players in facilitating tumor invasion and metastasis. Therefore, a high level of miR-494 plays an important role in regulating the activity of MDSCs in promotion of tumor progression and might be identified as a potential therapeutic target.

Discussion

Previous studies have revealed the existence of potentially widespread posttranscriptional regulatory mechanisms that have crucial roles in regulating the development and function of immune cells (29–31). The mediators of these processes are known as miRNAs, an abundant class of endogenous, small, noncoding RNAs that can form imperfect Watson–Crick bp at multiple sites within the 3′-UTR of their cognate mRNA targets to repress their expression (32, 33). miRNA dysregulation in immune cells can lead to various immune-related pathological disorders, such as inflammation and cancer (34). Accumulating evidence indicates that MDSCs expanded by TDFs are negative regulators for the anti-tumor immune responses. More importantly, they have remarkable nonimmunological activities that contribute to tumor progression (19, 23). A very recent study reported that miR-17-5p and miR-20a alleviated the immunosuppressive potential of MDSCs by modulating STAT3 expression (35). However, the molecular events controlling the accumulation and activation of tumor-expanded MDSCs are largely unknown, and it is also not clear whether and how noncoding RNAs are involved.

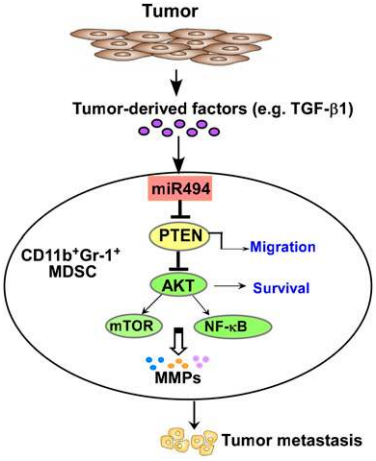

FIGURE 7. Working model of the conclusion that miR-494 promotes the accumulation and functions of MDSCs by regulating the PTEN/Akt pathway.

In this study, we reported that miR-494 expression was significantly increased in MDSCs derived from six different tumor models compared with the amount found in control cells. TCCM could markedly induce the expression of miR-494 in Gr-1$^+$ CD11b$^+$ cells in a dose-dependent manner. We identified TGF-β1 as one of the main factors responsible for the miR-494 upregulation. TGF-β plays an important role in tumor initiation and progression, functioning as both a suppressor and a promoter. It has been shown to inhibit epithelial cell proliferation and promote epithelial cell apoptosis. TGF-β1 transgenic mice are resistant to chemical carcinogen DMBA-induced mammary tumor formation (36). However, treatment of *TGF-β1* knockdown mice with chemical carcinogens resulted in enhanced tumorigenesis (37). Many studies have shown that TGF-β produced by tumor cells and various types of immune cells exerts critical roles in the negative regulation of host immunosurveillance (38). In addition to the suppressive effect on the proliferation and activation of effector immune cells, our results indicated that TGF-β1 released from tumor cells has forceful actions in regulating the functions of MDSCs by inducing miR-494 expression; this induction was dependent on the Smad 3 pathway. The fact that MDSCs can also produce TGF-β suggests a positive feedback loop that may act to amplify the effect of miR-494 on MDSCs.

Tumor-infiltrating MDSCs had significantly higher expression levels of miR-494, ARG1, and MMPs compared with those of splenic MDSCs, which might be partially due to the higher level of TDFs (e.g., TGF-β1) in the tumor microenvironment. The growth of the primary 4T1 tumors was reduced and lung metastasis was rarely detected when endogenous miR-494 activity was inhibited in vivo. Even when the depletion of CD8$^+$ T cells restored primary tumor growth, inhibition of miR-494 still significantly reduced the lung metastases; this, in combination with the data from the in vitro invasion assay, suggested that miR-494 governs the activity of MDSCs in facilitating tumor invasion and metastasis via regulating the expression of MMPs. The MMPs are a family of extracellular endopeptidases that can degrade virtually all extracellular matrix components (39). The MMPs have been implicated in the processes of tumor invasion and metastasis, and their overexpression is associated with an aggressive malignant phenotype and a poor prognosis in patients with cancer (40). The MMPs are also key regulators of the epithelial to mesenchymal transition, angiogenesis, and cancer-associated inflammation (41, 42). MMP14, one of the most studied MMPs, can activate pro-MMP2 and pro-MMP13, and the expression of MMP14 was colocalized with that of MMP2 and MMP-13 suggesting their contribution in a proteolytic cascade (43, 44). MMP-2 has been identified as a modulator that selectively mediates the lung metastasis of breast cancer (40). It has been recently emphasized that

most of the MMPs are predominantly produced by stromal cells and tumor-infiltrating inflammatory cells rather than cancer cells (45, 46). Yang et al. (11) have reported that tumor-infiltrating MDSCs produce multiple MMPs (MMP2, MMP13, MMP14) that significantly contribute to tumor invasion and metastasis; however, the mechanisms whereby the expression of these MMPs is controlled in MDSCs still remain unclear. In the current study, we provide a new insight that miR-494 in MDSCs could induce the expression of MMPs to promote tumor invasion and metastasis. Furthermore, a high level of miR-494 in MDSCs not only altered the intrinsic apoptotic/survival signal but also enhanced the efficiency of CXCR4-mediated recruitment and the immunosuppressive activity of MDSCs.

Recent studies have reported that the JAK/STAT signaling pathways play crucial roles in the biological activity of MDSCs, and STAT3 pathway is mainly involved in the regulation of the immunosuppressive function of MDSCs (8, 12, 47, 48). However, it is still not clear whether other signaling pathways are involved. As a tumor suppressor, a mutated or inactivated form of *PTEN* is frequently observed in a wide variety of human cancers (49). In addition to its tumor-suppressive function, PTEN also plays a critical role in the maintenance of the normal physiological functions of many organ systems. In the immune system, published work has shown that depending on the cell type, PTEN is important for proper development, cell fate, and cell function (50). Another important finding of the current study is that the PTEN/Akt pathway is critical in regulating the nonimmunological functions of tumor-expanded MDSCs. PTEN expression in MDSCs was suppressed by TDF-induced upregulation of miR-494, which enhanced the infiltration of MDSCs into the tumor site via the SDF-1/CXCR4 axis. Furthermore, downregulation of PTEN activated the PI3K/Akt pathway that alters the intrinsic apoptotic/survival signal to prolong the lifespan of MDSCs, which further contributed to the MDSC accumulation. More importantly, the activated PI3K/Akt pathway potently promotes the expression of MMPs to facilitate tumor cell invasion and metastasis.

In summary, we have demonstrated an important regulatory pathway in governing the accumulation and activation of tumor-associated MDSCs. miR-494 in MDSCs was upregulated by TDFs and played a critical role in promotion of tumor growth and metastasis by regulating the activity of MDSCs via targeting of PTEN, thereby resulting in the subsequent activation of the Akt, NF-κB, and mTOR pathways and induction of expression of MMPs. Targeting of miR-494 not only generates anti-tumor immunity but also inhibits tumor metastasis and thus might be explored as a potential therapeutic target.

Acknowledgments

We thank Dr. Linrong Lu, Dr. Zhijian Cai, and Dr. Di Wang for helpful discussions, Dr. Guili Hu and Yingying Huang for FACS sorting, and Dr. Hong Li (National Institute on Environmental Health Sciences) for critical reading of the manuscript.

Disclosures

The authors have no financial conflicts of interest.

References

1. Gallina, G., L. Dolcetti, P. Serafini, C. De Santo, I. Marigo, M. P. Colombo, G. Basso, F. Brombacher, I. Borrello, P. Zanovello, et al. 2006. Tumors induce a subset of inflammatory monocytes with immunosuppressive activity on CD8+ T cells. *J. Clin. Invest.* 116: 2777–2790.
2. Murdoch, C., M. Muthana, S. B. Coffelt, and C. E. Lewis. 2008. The role of myeloid cells in the promotion of tumour angiogenesis. *Nat. Rev. Cancer* 8: 618–631.
3. Pak, A. S., M. A. Wright, J. P. Matthews, S. L. Collins, G. J. Petruzzelli, and M. R. Young. 1995. Mechanisms of immune suppression in patients with head and neck cancer: presence of CD34(+) cells which suppress immune functions within cancers that secrete granulocyte-macrophage colony-stimulating factor. *Clin. Cancer Res.* 1: 95–103.
4. Gabrilovich, D. I., and S. Nagaraj. 2009. Myeloid-derived suppressor cells as regulators of the immune system. *Nat. Rev. Immunol.* 9: 162–174.
5. Youn, J. I., S. Nagaraj, M. Collazo, and D. I. Gabrilovich. 2008. Subsets of myeloid-derived suppressor cells in tumor-bearing mice. *J. Immunol.* 181: 5791–5802.
6. Movahedi, K., M. Guilliams, J. Van den Bossche, R. Van den Bergh, C. Gysemans, A. Beschin, P. De Baetselier, and J. A. Van Ginderachter. 2008. Identification of discrete tumor-induced myeloid-derived suppressor cell subpopulations with distinct T cell-suppressive activity. *Blood* 111: 4233–4244.
7. Bronte, V., and P. Zanovello. 2005. Regulation of immune responses by L-arginine metabolism. *Nat. Rev. Immunol.* 5: 641–654.
8. Condamine, T., and D. I. Gabrilovich. 2011. Molecular mechanisms regulating myeloid-derived suppressor cell differentiation and function. *Trends Immunol.* 32: 19–25.
9. Li, H., Y. Han, Q. Guo, M. Zhang, and X. Cao. 2009. Cancer-expanded myeloid-derived suppressor cells induce anergy of NK cells through membrane-bound TGF-beta 1. *J. Immunol.* 182: 240–249.
10. Zhang, Y., Q. Liu, M. Zhang, Y. Yu, X. Liu, and X. Cao. 2009. Fas signal promotes lung cancer growth by recruiting myeloid-derived suppressor cells via cancer cell-derived PGE2. *J. Immunol.* 182: 3801–3808.
11. Yang, L., J. Huang, X. Ren, A. E. Gorska, A. Chytil, M. Aakre, D. P. Carbone, L. M. Matrisian, A. Richmond, P. C. Lin, and H. L. Moses. 2008. Abrogation of TGF beta signaling in mammary carcinomas recruits Gr-1+CD11b+ myeloid cells that promote metastasis. *Cancer Cell* 13: 23–35.
12. Chalmin, F., S. Ladoire, G. Mignot, J. Vincent, M. Bruchard, J. P. Remy-Martin, W. Boireau, A. Rouleau, B. Simon, D. Lanneau, et al. 2010. Membrane-associated Hsp72 from tumor-derived exosomes mediates STAT3-dependent immunosuppressive function of mouse and human myeloid-derived suppressor cells. *J. Clin. Invest.* 120: 457–471.
13. Bushati, N., and S. M. Cohen. 2007. microRNA functions. *Annu. Rev. Cell Dev. Biol.* 23: 175–205.
14. Ma, F., X. Liu, D. Li, P. Wang, N. Li, L. Lu, and X. Cao. 2010. MicroRNA-466l upregulates IL-10 expression in TLR-triggered macrophages by antagonizing RNA-binding protein tristetraprolin-mediated IL-10 mRNA degradation. *J. Immunol.* 184: 6053–6059.
15. Liu, Y., Q. Chen, Y. Song, L. Lai, J. Wang, H. Yu, X. Cao, and Q. Wang. 2011. MicroRNA-98 negatively regulates IL-10 production and endotoxin tolerance in macrophages after LPS stimulation. *FEBS Lett.* 585: 1963–1968.
16. Yang, X., J. J. Letterio, R. J. Lechleider, L. Chen, R. Hayman, H. Gu, A. B. Roberts, and C. Deng. 1999. Targeted disruption of SMAD3 results in impaired mucosal immunity and diminished T cell responsiveness to TGF-beta. *EMBO J.* 18: 1280–1291.
17. Hong, X., Y. Liu, G. Hu, D. Zhao, J. Shen, F. Shen, X. Cao, and Q. Wang. 2009. EBAG9 inducing hyporesponsiveness of T cells promotes tumor growth and metastasis in 4T1 murine mammary carcinoma. *Cancer Sci.* 100: 961–969.
18. Wang, Q. Q., H. Li, T. Oliver, M. Glogauer, J. Guo, and Y. W. He. 2008. Integrin beta 1 regulates phagosome maturation in macrophages through Rac expression. *J. Immunol.* 180: 2419–2428.
19. Cheng, P., C. A. Corzo, N. Luetteke, B. Yu, S. Nagaraj, M. M. Bui, M. Ortiz, W. Nacken, C. Sorg, T. Vogl, et al. 2008. Inhibition of dendritic cell differentiation and accumulation of myeloid-derived suppressor cells in cancer is regulated by S100A9 protein. *J. Exp. Med.* 205: 2235–2249.
20. Rodriguez, P. C., C. P. Hernandez, D. Quiceno, S. M. Dubinett, J. Zabaleta, J. B. Ochoa, J. Gilbert, and A. C. Ochoa. 2005. Arginase I in myeloid suppressor cells is induced by COX-2 in lung carcinoma. *J. Exp. Med.* 202: 931–939.
21. Serafini, P., I. Borrello, and V. Bronte. 2006. Myeloid suppressor cells in cancer: recruitment, phenotype, properties, and mechanisms of immune suppression. *Semin. Cancer Biol.* 16: 53–65.
22. Yang, L., C. M. Edwards, and G. R. Mundy. 2010. Gr-1+CD11b+ myeloid-derived suppressor cells: formidable partners in tumor metastasis. *J. Bone Miner. Res.* 25: 1701–1706.
23. Marigo, I., E. Bosio, S. Solito, C. Mesa, A. Fernandez, L. Dolcetti, S. Ugel, N. Sonda, S. Bicciato, E. Falisi, et al. 2010. Tumor-induced tolerance and immune suppression depend on the C/EBPbeta transcription factor. *Immunity* 32: 790–802.
24. Zhu, D., H. Hattori, H. Jo, Y. Jia, K. K. Subramanian, F. Loison, J. You, Y. Le, M. Honczarenko, L. Silberstein, and H. R. Luo. 2006. Deactivation of phosphatidylinositol 3,4,5-trisphosphate/Akt signaling mediates neutrophil spontaneous death. *Proc. Natl. Acad. Sci. USA* 103: 14836–14841.
25. Gao, P., R. L. Wange, N. Zhang, J. J. Oppenheim, and O. M. Howard. 2005. Negative regulation of CXCR4-mediated chemotaxis by the lipid phosphatase activity of tumor suppressor PTEN. *Blood* 106: 2619–2626.
26. Ohno, S., H. J. Im, C. B. Knudson, and W. Knudson. 2006. Hyaluronan oligosaccharides induce matrix metalloproteinase 13 via transcriptional activation of NFkappaB and p38 MAP kinase in articular chondrocytes. *J. Biol. Chem.* 281: 17952–17960.
27. Zhang, D., and P. Brodt. 2003. Type 1 insulin-like growth factor regulates MT1-MMP synthesis and tumor invasion via PI 3-kinase/Akt signaling. *Oncogene* 22: 974–982.
28. Kato, M., S. Putta, M. Wang, H. Yuan, L. Lanting, I. Nair, A. Gunn, Y. Nakagawa, H. Shimano, I. Todorov, et al. 2009. TGF-beta activates Akt kinase through a microRNA-dependent amplifying circuit targeting PTEN. *Nat. Cell Biol.* 11: 881–889.
29. Baltimore, D., M. P. Boldin, R. M. O'Connell, D. S. Rao, and K. D. Taganov. 2008. MicroRNAs: new regulators of immune cell development and function. *Nat. Immunol.* 9: 839–845.

30. Xiao, C., and K. Rajewsky. 2009. MicroRNA control in the immune system: basic principles. *Cell* 136: 26–36.
31. Rodriguez, A., E. Vigorito, S. Clare, M. V. Warren, P. Couttet, D. R. Soond, S. van Dongen, R. J. Grocock, P. P. Das, E. A. Miska, et al. 2007. Requirement of bic/microRNA-155 for normal immune function. *Science* 316: 608–611.
32. Bartel, D. P. 2004. MicroRNAs: genomics, biogenesis, mechanism, and function. *Cell* 116: 281–297.
33. Lodish, H. F., B. Zhou, G. Liu, and C. Z. Chen. 2008. Micromanagement of the immune system by microRNAs. *Nat. Rev. Immunol.* 8: 120–130.
34. Pedersen, I. M., G. Cheng, S. Wieland, S. Volinia, C. M. Croce, F. V. Chisari, and M. David. 2007. Interferon modulation of cellular microRNAs as an antiviral mechanism. *Nature* 449: 919–922.
35. Zhang, M., Q. Liu, S. Mi, X. Liang, Z. Zhang, X. Su, J. Liu, Y. Chen, M. Wang, Y. Zhang, et al. 2011. Both miR-17-5p and miR-20a alleviate suppressive potential of myeloid-derived suppressor cells by modulating STAT3 expression. *J. Immunol.* 186: 4716–4724.
36. Pierce, D. F., Jr., A. E. Gorska, A. Chytil, K. S. Meise, D. L. Page, R. J. Coffey, Jr., and H. L. Moses. 1995. Mammary tumor suppression by transforming growth factor beta 1 transgene expression. *Proc. Natl. Acad. Sci. USA* 92: 4254–4258.
37. Tang, B., E. P. Böttinger, S. B. Jakowlew, K. M. Bagnall, J. Mariano, M. R. Anver, J. J. Letterio, and L. M. Wakefield. 1998. Transforming growth factor-beta1 is a new form of tumor suppressor with true haploid insufficiency. *Nat. Med.* 4: 802–807.
38. Yang, L., Y. Pang, and H. L. Moses. 2010. TGF-beta and immune cells: an important regulatory axis in the tumor microenvironment and progression. *Trends Immunol.* 31: 220–227.
39. Page-McCaw, A., A. J. Ewald, and Z. Werb. 2007. Matrix metalloproteinases and the regulation of tissue remodelling. *Nat. Rev. Mol. Cell Biol.* 8: 221–233.
40. Minn, A. J., G. P. Gupta, P. M. Siegel, P. D. Bos, W. Shu, D. D. Giri, A. Viale, A. B. Olshen, W. L. Gerald, and J. Massagué. 2005. Genes that mediate breast cancer metastasis to lung. *Nature* 436: 518–524.
41. Radisky, D. C., D. D. Levy, L. E. Littlepage, H. Liu, C. M. Nelson, J. E. Fata, D. Leake, E. L. Godden, D. G. Albertson, M. A. Nieto, et al. 2005. Rac1b and reactive oxygen species mediate MMP-3-induced EMT and genomic instability. *Nature* 436: 123–127.
42. Mitsiades, N., W. H. Yu, V. Poulaki, M. Tsokos, and I. Stamenkovic. 2001. Matrix metalloproteinase-7-mediated cleavage of Fas ligand protects tumor cells from chemotherapeutic drug cytotoxicity. *Cancer Res.* 61: 577–581.
43. Knäuper, V., H. Will, C. López-Otin, B. Smith, S. J. Atkinson, H. Stanton, R. M. Hembry, and G. Murphy. 1996. Cellular mechanisms for human procollagenase-3 (MMP-13) activation. Evidence that MT1-MMP (MMP-14) and gelatinase a (MMP-2) are able to generate active enzyme. *J. Biol. Chem.* 271: 17124–17131.
44. Bisson, C., S. Blacher, M. Polette, J. F. Blanc, F. Kebers, J. Desreux, B. Tetu, J. Rosenbaum, J. M. Foidart, P. Birembaut, and A. Noel. 2003. Restricted expression of membrane type 1-matrix metalloproteinase by myofibroblasts adjacent to human breast cancer cells. *Int. J. Cancer* 105: 7–13.
45. Hidalgo, M., and S. G. Eckhardt. 2001. Development of matrix metalloproteinase inhibitors in cancer therapy. *J. Natl. Cancer Inst.* 93: 178–193.
46. Chabottaux, V., and A. Noel. 2007. Breast cancer progression: insights into multifaceted matrix metalloproteinases. *Clin. Exp. Metastasis* 24: 647–656.
47. Sinha, P., V. K. Clements, and S. Ostrand-Rosenberg. 2005. Interleukin-13-regulated M2 macrophages in combination with myeloid suppressor cells block immune surveillance against metastasis. *Cancer Res.* 65: 11743–11751.
48. Delano, M. J., P. O. Scumpia, J. S. Weinstein, D. Coco, S. Nagaraj, K. M. Kelly-Scumpia, K. A. O'Malley, J. L. Wynn, S. Antonenko, S. Z. Al-Quran, et al. 2007. MyD88-dependent expansion of an immature GR-1(+)CD11b(+) population induces T cell suppression and Th2 polarization in sepsis. *J. Exp. Med.* 204: 1463–1474.
49. Cantley, L. C., and B. G. Neel. 1999. New insights into tumor suppression: PTEN suppresses tumor formation by restraining the phosphoinositide 3-kinase/AKT pathway. *Proc. Natl. Acad. Sci. USA* 96: 4240–4245.
50. Knobbe, C. B., V. Lapin, A. Suzuki, and T. W. Mak. 2008. The roles of PTEN in development, physiology and tumorigenesis in mouse models: a tissue-by-tissue survey. *Oncogene* 27: 5398–5415.